

Fabrication by AC Deposition and Antimicrobial Properties of Pyramidal-Shaped $\text{Cu}_2\text{O-TiO}_2$ Heterostructures

Regular Paper

Rokas Žalneravičius¹, Algimantas Paškevičius¹, Jelena Kovger¹ and Arūnas Jagminas^{1*}

¹ Centre for Physical Sciences and Technology, Institute of Chemistry, Vilnius, Lithuania
Institute of Botany of Nature Research Centre, Vilnius, Lithuania

* Corresponding author(s) E-mail: jagmin@ktl.mii.lt

Received 03 July 2014; Accepted 27 Oct 2014

DOI: 10.5772/59997

© 2014 The Author(s). Licensee InTech. This is an open access article distributed under the terms of the Creative Commons Attribution License (<http://creativecommons.org/licenses/by/3.0>), which permits unrestricted use, distribution, and reproduction in any medium, provided the original work is properly cited.

Abstract

Nanoparticulate surfaces possessing antimicrobial and fungicidal properties under visible light illumination have found wide applications in a number of fields. In this study, titania nanotubes, as well as titania compact films were designed with pure Cu_2O crystals in a mildly acidic copper acetate solution using a simple alternating current (AC) deposition approach. In this way, the thermally oxidized Ti substrate was coated by densely packed pyramidal and bi-pyramidal shaped Cu_2O crystals with dominant (111) planes and investigated against several types of fungi and bacteria. For comparison, TiO_2 nanotube (TiNT) films were also decorated with similar crystals and tested. The results showed that, compared to bare TiO_2 films, both Cu_2O -in-TiNT and Cu_2O -on- TiO_2 heterostructures exhibited remarkably enhanced activity against tested fungi and bacteria. We also demonstrated that the high photoactivity of these crystals remained even after 50 h stability tests under bright light illumination. The results obtained from in vitro tests indicated that Cu_2O -in/on- TiO_2 heterostruc-

tures show promise as visible light driven antimicrobial materials.

Keywords nanocomposite, titania nanotube films, cuprous oxide, antimicrobial

1. Introduction

Titanium (Ti), due to its high mechanical hardness, low density, elevated chemical stability, relatively low cost, environmentally-friendly characteristics and photocatalytic activity under UV irradiation, belongs to the category of metals suitable for the production of orthopaedic and dental implants, surgical instruments and self-cleaning surfaces. In air, this metal is always covered by a thin TiO_2 film, the thickness of which can be increased simply by thermal and chemical oxidation or anodization high up in the sub- μm scale. TiO_2 films produced by anodizing/

annealing may vary in terms of electronic and phase structure (anatase, brookite, rutile) porosity and activity [1]. Due to a large band gap energy (~3.2 eV) and a more positive conduction band potential than the potential required for water reduction (1.23 V *vs.* NHE at pH = 0), pure TiO₂ films effectively absorb light, split water and demonstrate self-cleaning properties under UV light illumination [2, 3]. The antibacterial behaviour of UV illuminated TiO₂ powders were first reported three decades ago [4]. Recent reports on the bactericidal properties of various TiO₂ nanoparticles and films are frequently based on pure TiO₂ photocatalytic behaviour under UV irradiation [5]. Many studies have also been devoted to the formation of TiO₂-based bactericide particles under visible-light illumination [6-9]. For example, the solvothermal approach has been proposed for the synthesis of various Cu₂O crystals, indicating that the obtained Cu₂O crystals show good antibacterial effects and that with the morphology of the Cu₂O crystals changing from cubic to octahedral, their antibacterial properties change from general bacteriostasis to high selectivity [10]. Dispersed in the tested solutions, these photocatalysts have shown promising bactericidal effects under visible light irradiation. However, in all of these applications, the post-separation of doped TiO₂ species from the disinfected solutions are required. This procedure is tedious and cost-intensive, rendering it unsuitable for the cleaning of drinking water.

In the past decade, to avoid the cleaning of tested solutions, immobilization of the TiO₂-based photocatalyst species onto various substrates have been proposed [11-14]. For example, CNT-doped TiNT on glass by dip-coating [11], Ag/TiO₂ composite films [12], CdS/Pt-TiNT [13] and high-efficient CdS/TiNT films [14] on the Ti substrate have been reported. However, most of these surfaces showed either low-effectiveness under illumination by bright light or were toxic due to the application of CdS.

Currently, several routes have been also reported for TiO₂ conduction and valence band re-design, for example, via attachment of non-toxic lower band gap semiconducting nanoparticles, such as Cu₂O [14, 15] and CuO [16, 17].

Cuprous oxide (Cu₂O) is typically a *p*-type semiconductor possessing a direct band gap of 2.0-2.2 eV [18]. Owing to visible light absorption, chemical and physical stability, and its low cost, nanostructured Cu₂O particle arrays have recently drawn significant interest in terms of the photo conversion of bright light into electrical or chemical energy [15, 19, 20]. Note that solar conversion efficiency is equal to 11% from the theoretically possible [21]. In addition, recent studies have implied that Cu₂O crystallites demonstrated distinctive antimicrobial activity against some types of bacteria [22,23]. According to Lu et al. [10], the antimicrobial activity of Cu₂O crystallites, including cubic, octahedral, hexa-spindel, polyhedral, etc., depended on their morphology. All of these crystallites demonstrated antibactericidal activity, but only octahedral-shaped ones possessed high selectivity. Furthermore, it has recently

been reported that polycrystalline Cu₂O with four-sided pyramidal shape species that electrodeposited onto the ITO glass substrate, in contrast to single-crystal *p*-Cu₂O ones [24, 25], were quite stable in aqueous solutions under visible light illumination [26, 27]. This stability was linked to the predominant Cu⁺-termination of (111) planes of electrodeposited *p*-Cu₂O, at which the reduction of Cu₂O to Cu⁰ by reaction $\text{Cu}_2\text{O} + \text{H}_2\text{O} + 4\text{e}^- \rightarrow 2\text{Cu}^0 + 2\text{OH}^-$ did not take place [27]. It was therefore suspected that if well-attached to the titanium oxide substrate, numerous pyramidal Cu₂O crystallites with (111) planes could provide stable fungicidal and antimicrobial activity under visible light illumination.

The aim of this study was to design TiO₂/Cu₂O heterostructured films onto the titanium substrate possessing high stability and effective antimicrobial properties against several types of fungi and bacteria under solar light illumination. To achieve this result, an aqueous solution comprising Cu(II) acetate, Mg acetate and acetic acid at a pH = 5.3, as well as an alternating current approach, are proposed in this study. For comparison, polyhedral- and pyramidal-shaped Cu₂O crystals with (111) prevailing surfaces were organized both inside the TiO₂ nanotube (TiNT) film and onto the TiO₂ substrate. The stability of Cu₂O species tethered to the thermally oxidized Ti surface was investigated in a 0.5 mol L⁻¹ Na₂SO₄ aqueous solution at -0.35 V (*vs.* Ag/AgCl, sat.) and 100 W tungsten lamp illumination for 50 h. The antimicrobial properties of the obtained Cu₂O/TiO₂ heterostructures were tested against several types of fungi and bacteria.

2. Experimental

2.1 Reagents

A 98% purity copper acetate, Cu(CH₃COO)₂•H₂O, 99% purity magnesium acetate, Mg(CH₃COO)₂•4H₂O and 99% purity ammonium hepta molibdate, (NH₄)₆Mo₇O₂₄•4H₂O, were purchased from Sigma Aldrich. NaOH (98.8%), acetone (99.8%), ethylene glycol (99%) and acetic acid, CH₃COOH (99.8%) were obtained from Eurochemicals, Slovakia. Ammonium fluoride (98% purity) was obtained from Merck.

Saccharomyces cerevisiae, *Aspergillus versicolor*, *Candida parapsilosis* and *Candida krusei* fungi and *Pseudomonas aeruginosa*, *Escherichia coli*, and *Micrococcus luteus* bacteria were obtained from the Liofilchem (Italy).

2.2 Electrochemical formation of TiNT films

Ti foil at 99.7% purity and 0.127 mm thick and purchased from Aldrich was used to prepare disc-shaped specimens 13.8 mm in diameter. The surface of samples was ultrasonically cleaned in acetone, ethanol and water, for 6 min in each, air dried and anodized in the thermostated glass cell containing ethylene glycol (Etg) with 0.3% wt. NH₄F and 20 mL L⁻¹ H₂O at 20±1°C and 50 V using a DC power supply

for 40 min. To decrease the thickness of the titania barrier-layer, the anodizing voltage was decreased at the end of anodizing at a 1.0 V min^{-1} rate down to 30 V. Two platinum plates were maintained at a distance of 13 mm from the Ti specimen as cathodes. Each sample was anodized in a fresh solution. Resulting films were calcined in air at 450°C for 2 hrs using a $10^\circ\text{C min}^{-1}$ ramp and were also subjected to alternating current (AC) treatment. TiO_2 compact films were obtained via thermal oxidation of Ti specimens in air at 450°C for 2 hrs using a $10^\circ\text{C min}^{-1}$ ramp.

2.3 Electrodeposition of Cu_2O species

Electrodepositions of Cu_2O on TiO_2 nanotube walls and TiO_2 surface were accomplished in a two-electrode glass cell, in a 200 mL volume and containing an aqueous solution of 0.1 mol L^{-1} copper acetate, $\text{Cu}(\text{CH}_3\text{COO})_2 \cdot \text{H}_2\text{O}$, 0.1 mol L^{-1} magnesium acetate, $\text{Mg}(\text{CH}_3\text{COO})_2 \cdot 4\text{H}_2\text{O}$ and acetic acid. Based on previous investigations [28], $\text{Mg}(\text{II})$ salt was used to prevent the breakdown of the titania barrier layer during AC treatment. Several graphite stripes connected and positioned around the working specimen were used as a counter electrode. All depositions were carried out in a room temperature solution. Milli-Q water ($18 \text{ M}\Omega$) was used for the preparation of the Cu_2O deposition solution. Analytical grade $\text{Mg}(\text{OOCCH}_3)_2$, $\text{Cu}(\text{OOCCH}_3)_2$ and acetic acid were purchased from Eurochemicals Ltd. Owing to the rectifying properties of the titania barrier layer [29], the depositions were carried out by AC at a constant peak-to-peak voltage ($U_{\text{p-to-p}}$) mode using a programmable alternating current source Chroma AC (model 61602, Taiwan). The frequency of AC was varied within the 25 to 500 Hz range. All solutions were prepared with deionized water and reagent grade chemicals. After deposition, each sample was thoroughly rinsed with pure water and air dried.

2.4 Characterization

To ascertain the purity of Cu_2O species tethered to the TiNT walls, voltammetric measurements were performed using a potentiostat/galvanostat AUTOLAB 302 and a three-electrode electrochemical cell, in which Pt wire and a hydrogen electrode were used in the working solution (RHE) as a counter and reference electrodes, respectively. Prior to measurements, a working solution composed of 0.1 mol L^{-1} KOH was de-aerated by Ar gas bubbling for at least 0.5 h.

The stability tests of Cu_2O crystals tethered to the TiO_2 surface was carried out in 0.5 mol L^{-1} Na_2SO_4 solution under $\sim 10 \text{ mW cm}^{-2}$ irradiation provided by 100 W tungsten arc lamp illumination potentiostatically at -0.35 V (*vs.* Ag/AgCl, sat.) for up to 50 hrs. The content of Cu_2O and Cu deposited (and dissolved during stability tests) was determined by the analysis of solutions, obtained via etching the specimens in a hot $\text{HNO}_3\text{:H}_2\text{O}$ (1:1) solution followed by careful rinsing and sonication in Milli-Q water.

The inductively coupled plasma emission spectrometer OPTIMA 7000DV (Perkin Elmer, USA) was employed for analysis. Measurements were made on emission peaks at 327.393 and 324.752 nm for Cu, at least five times for the same solution.

To examine the morphology of films on the surface and in cross-sections, a scanning electron microscope, model FEI Quatra 200F and a Cross Beam Workstation Auriga, equipped with a field emission gun and EDX spectrometer were used.

Phase composition of the obtained heterostructures was studied by X-ray powder diffraction (XRD) using a D8 diffractometer (Bruker AXS, Germany), equipped with a Göbel mirror as a primary beam monochromator for CuK_α radiation. A step-scan mode was used in the 2θ range from 18 to 77° with a step-length of 0.02° and a counting time of 8 s per step. The size of crystallites was determined from the broadening of all diffraction peaks using PDXL software and Halder-Wagner (H-W) approximation.

Raman spectra were recorded using an inVia (Renishaw) spectrometer equipped with a thermoelectrically cooled (-70°C) CCD camera and microscope. The 532 nm solid state diode laser beam was used as an excitation source. The laser power at the sample was restricted to 0.06 mW and 0.6 mW for samples Ti oxide/ Cu_2O and bare Ti oxide, respectively. The Raman scattering wavenumber axis was calibrated by the silicon peak at 520.7 nm. The spectral slit width near 500 cm^{-1} was 6.7 cm^{-1} . The 50x objective was used during all measurements. The laser line was focused to a $\sim 2 \mu\text{m}$ diameter spot on the sample. The parameters of bands were determined by fitting the experimental spectra with Gaussian-Lorentzian shape components using GRAMS/A1 8.0 (Thermo Scientific) software.

The antibacterial effects of the fabricated films were assessed using the *Saccharomyces cerevisiae*, *Aspergillus versicolor*, *Cladosporium cladosporioides*, *Candida parapsilosis* and *Candida krusei* fungi, cultured in Sabouraud CAF agar at 27°C , and *Pseudomonas aeruginosa*, *Escherichia coli* and *Micrococcus luteus* bacteria cultured in Nutrient agar at 27°C , and the effects on colony-forming units were analysed.

The antimicrobial activity of Cu_2O -in/on-TiNT samples against *Micrococcus luteus* (*M. luteus*), *Escherichia coli* (*E. coli*), *Aspergillus fumigatus* (*A. fumigatus*), *Geotrichum candidum* (*G. candidum*) and *Candida parapsilosis* (*C. parapsilosis*) was investigated using the zone inhibition method. Following this method, the pieces of alumina films were pressed gently onto Sabouraud CAF agar or Nutrient-agar ("Liofilchem", Italy) plates inoculated with $\geq 10^6 \text{ CFU mL}^{-1}$ microorganisms and analysed after 48 h incubation at $27 \pm 1^\circ\text{C}$.

It should be noted that unless otherwise indicated, all the above-mentioned experiments were repeated three times and the obtained results were statistically analysed by

calculating averages and standard deviations. The resulting data were applied for building corresponding diagrams.

3. Results and discussion

3.1 Composition and structure of heterostructured films

We have reported recently that TiNT walls can be decorated with numerous pure Cu_2O species both inside and outside tubes *via* alternating current deposition from a slightly acidic Cu(II) acetate solution (Fig.1 A, B) [29]. The size of crystallites increased with the deposition bath voltage and AC treatment time attaining 60 nm. In this study, we demonstrate that the same solution can be successfully explored for the formation of densely packed pyramidal- and bi-pyramidal-shaped (octahedral) Cu_2O crystals onto the thermally oxidized Ti substrate (Figures 1C and D). The shape of crystallites was found to be dependent on the pH of solution and AC deposition conditions, similar to the case of potentiostatic depositions from the alkaline cupric lactate solution onto the ITO substrate [27]. The pH of solution kept at a pH within 5.2 to 5.35 range was found to be an optimal. In this solution, by variables in the AC treatment conditions (U_{p-to-p} value, AC frequency and deposition time) the surface of the thermally oxidized Ti substrate can be predictably covered with densely packed pyramidal-shaped crystallites (Fig. 1C). The planar dimensions of the pyramidal and bi-pyramidal crystals were found to be dependent mainly on the AC treatment time and U_{p-to-p} value, attaining sub-micrometre size. Most uniform covering of TiO_2 surface took place at 100 Hz frequency although some higher deposition rates were observed at 50 Hz frequency (Figure 2). Please note that randomly dispersed crystals can be formed at up to 250 Hz frequency. The shape of the deposited species depends on the pH of the solution although the pyramidal-shaped species can be deposited only from slightly acidic acetate solutions (Figure 3A). In the neutral solutions, e.g. at around pH = 7.0, the coral-shaped species (Figure 3B) were formed, whereas in the alkaline solutions, e.g. at pH = 10.0 (Figure 3C) the nanoparticulate species dominated.

XRD and Raman investigations were used to characterize the phase structures of the deposited species. Figure 4 shows the XRD patterns of the $\text{Cu}_2\text{O}/\text{TiNT}$ heterostructure (A) and Cu_2O octahedra obtained by AC deposition from a slightly acidic Cu(II) acetate solution on the thermally oxidized Ti substrate (B). As can be seen, both XRD patterns contain several obvious diffraction peaks at 2θ positions 29.58, 36.42, 42.32, 61.46 and 73.60 that, according to PDF card no 01-078-2076, can be indexed as (110), (111), (200), (220), and (311) planes of the cubic phase cuprous oxide, allowing us to deduce that the deposited species are polycrystalline Cu_2O . It is also obvious that the preferred orientation of Cu_2O grains is (111). The size of Cu_2O grains calculated from the main diffraction line (111) broadening

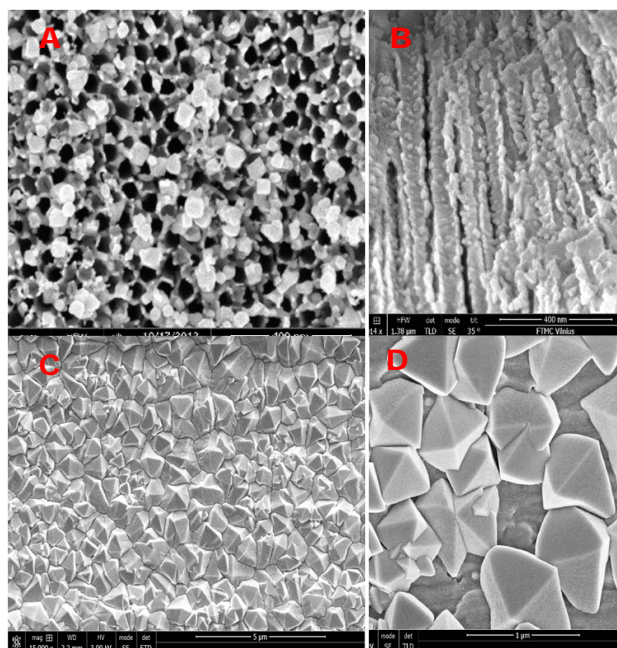


Figure 1. Top-side (A) and cross-sectional (B) SEM views of TiNT film fabricated by Ti anodizing in ethylene glycol solution, then annealed at 450 °C for 2 h and AC treated in Cu(II) acetate electrolyte at $U_{p-to-p} = 1.1$ V for 5 min. In (C) and (D): typical top-side SEM views of crystallites formed onto the thermally oxidized Ti substrate by AC deposition in the same solution at $U_{p-to-p} = 1.3$ V for 10 min

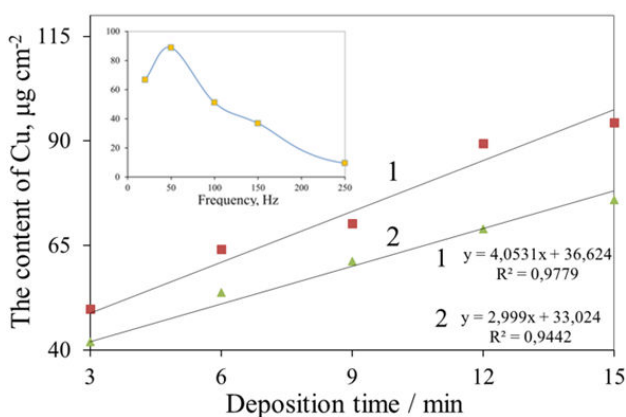


Figure 2. Variations of the content of deposited copper suboxide species onto the thermally oxidized Ti substrate in the solution comprising 0.1 mol L^{-1} $\text{Cu(OOCCH}_3)_2$ + 0.1 mol L^{-1} $\text{Mg(OOCCH}_3)_2$ + CH_3COOH (pH = 5.3) at $U_{p-to-p} = 1.3$ V and AC frequency: (1) 50, (2) 100 Hz on the deposition time. In the *Inset*: the dependency of deposited copper at $U_{p-to-p} = 1.3$ V for 10 min on the AC frequency

was found to be dependent on the conditions of electrodeposition varying within 32-45 and 65-85 nm ranges for Cu_2O species deposited inside the TiNT and onto the TiO_2 substrate, respectively. No peaks that can be ascribed to CuO or Cu(OH)_2 were detected, although two small peaks at 2θ positions around 43.3° and 50.4° (Figure 4B) could be linked with the presence of some Cu^0 onto the heat-treated Ti surface. It is also obvious that the pattern of TiNT film demonstrating a set of 10 reflections as shown in Figure 4A by the blue stars, according to PDF card no 00-021-1272,

indicated the presence of TiNT in the anatase-TiO₂ phase, whereas these peaks are absent in the heat-treated specimen.

Figure 5A compares the Raman spectra of the TiNT film before and after deposition of copper containing species. Strong Raman bands at 147, 397, 518, and 637 cm⁻¹ are characteristic of crystalline anatase TiO₂ structure [30, 31] whereas difference spectrum (c) clearly shows several peaks associated with copper oxygenous compounds. In brief, bands at 219, 533, and 625 cm⁻¹ evidence the presence of Cu₂O [32-34]. The Raman spectrum of pure thermally oxidized Ti substrate corresponds to the rutile TiO₂ phase with characteristic E_g and A_{1g} modes at 444 and 609 cm⁻¹, respectively (Figure 5B) [31], whereas bands at 98, 215, 531, and 617 cm⁻¹ according to [33-35] evidence the presence of Cu₂O.

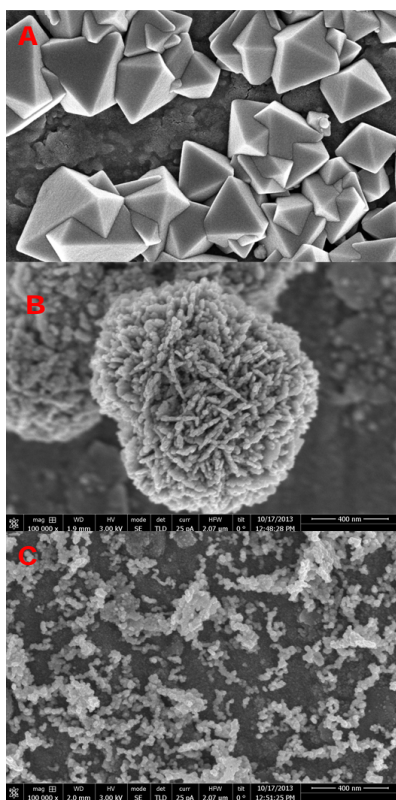


Figure 3. Top-side FESEM views of crystallites formed onto the thermally oxidized Ti substrate by AC deposition at $U_{p-to-p} = 1.3$ V and room temperature for 10 min in the same way as in Figure 2 with the solution kept at the pH: (A) 5.0; (B) 7.0 and (C) 10.0

The purity tests for AC-deposited Cu₂O pyramidal crystals were further performed in a 0.1 mol L⁻¹ KOH de-aerated solution by potential sweep from the open circuit potential, e.g. 0.75 V versus RHE, to -0.25 V and backwards. Voltammograms obtained for different contents of deposited species are shown in Figure 6. As seen, only a sharp reduction peak at ~-0.1 V, attributable to Cu₂O reduction is characteristic for all specimens. According to [36], such a reduction plot indicates the presence of pure Cu₂O.

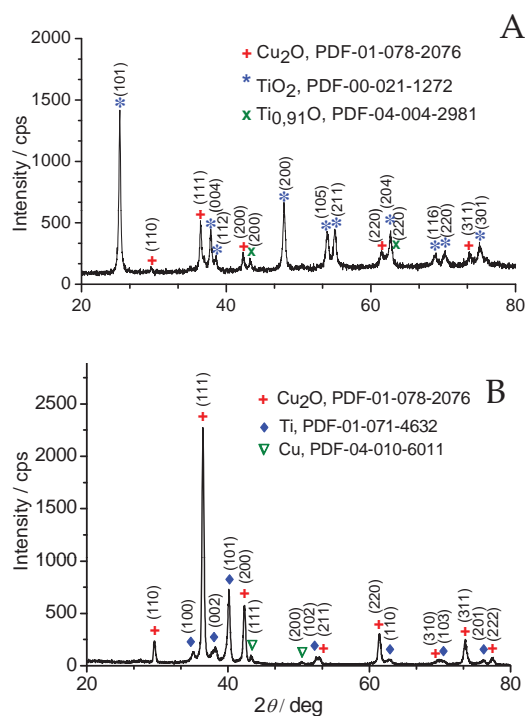


Figure 4. Typical XRD patterns (A) (B) of Cu₂O species deposited inside the TiNT film (A) and on the heat-treated TiO₂ substrate (B) by AC (100 Hz) treatment in the solution as in Figure 2 at $U_{p-to-p} = 1.2$ V for 15 min

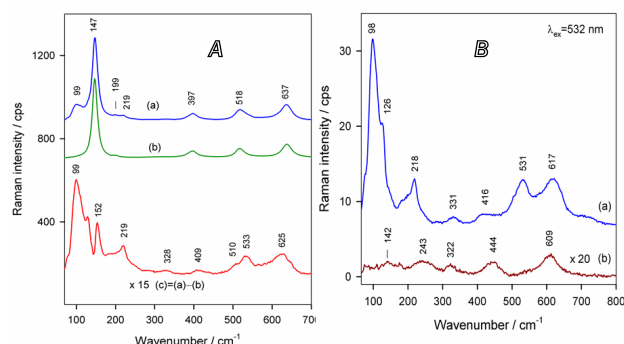


Figure 5. In (A): the Raman spectra of Cu₂O-in-TiNT (a), pure TiNT (b) and their difference (c) in wavenumber region from 65 to 700 cm⁻¹. In (B): the same for the Cu₂O deposited on the thermally oxidized Ti surface (a) and pure heat-treated Ti (b). Excitation wavelength is 532 nm. The same conditions as in Figure 4 were used for sample preparation.

3.2 Antimicrobial properties

The antibacterial activity results revealed that the pyramidal-shaped Cu₂O crystals encasing both the inside of the TiNT film tubes and deposited onto the rutile TiO₂ surface acted as excellent antimicrobial agents against all tested fungi as well as Gram-positive and Gram-negative bacterial strains. It should be noted that in the case of Cu₂O-on-rutile a fungistatic effect was observed for *A. versicolor* and *C. parapsilosis* fungi, whereas in the case of Cu₂O-in-TiNT the fungistatic effect was obtained in the Petri dishes with *A. versicolor*, *C. parapsilosis* and *C. krusei* strains. Figures 7 and 8 show the zones of inhibition produced by Cu₂O-in-

TiNT and Cu₂O-on-rutile TiO₂ against various eukaryotic and prokaryotic microorganism strains, respectively. Based on these results, some stronger fungicidal effects are characteristic for Cu₂O-on-rutile TiO₂ specimens showing the inhibition zones up to 25-27 mm after 48 h incubation (Table 1).

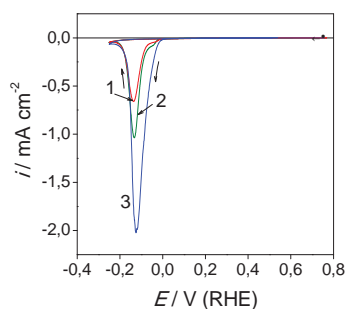


Figure 6. Reduction profiles of Cu₂O species deposited on the TiO₂ substrate by AC (100 Hz) treatment in the solution as in Figure 2, kept at a pH = 5.25 and $U_{p-to-p} = 1.2$ V for 5 (1), 10 (2) and 15 min (3). Voltammograms were recorded in the O₂-free 0.1 mol L⁻¹ KOH solution at $v = 1.0$ mV s⁻¹ and 20°C.

Microorganism	Antimicrobial agent	Disc potency (μg)	Diameter of disc (d) (mm)	Diameter of zone (z) (mm)	z/d
<i>Saccharomyces cerevisiae</i> ^a	Cu ₂ O-in-TiNT	33	14	25	1.8 ± 0.1
	Cu ₂ O-on-TiO ₂	114	14	27	1.9 ± 0.1
<i>Aspergillus versicolor</i> ^b	Cu ₂ O-in-TiNT	33	14	19	1.3 ± 0.2
	Cu ₂ O-on-TiO ₂	114	14	24	1.7 ± 0.2
<i>Candida parapsilosis</i> ^c	Cu ₂ O-in-TiNT	33	14	17	1.2 ± 0.1
	Cu ₂ O-on-TiO ₂	114	14	18	1.3 ± 0.1
<i>Candida krusei</i> ^d	Cu ₂ O-in-TiNT	33	14	18	1.3 ± 0.1
<i>Pseudomonas aeruginosa</i> ^e	Cu ₂ O-in-TiNT	33	14	25	1.8 ± 0.2
	Cu ₂ O-on-TiO ₂	114	14	24	1.7 ± 0.1
<i>Escherichia coli</i> ^f	Cu ₂ O-in-TiNT	33	14	15.5	1.1 ± 0.1
	Cu ₂ O-on-TiO ₂	114	14	15.5	1.1 ± 0.1
<i>Micrococcus luteus</i> ^g	Cu ₂ O-in-TiNT	33	14	16	1.1 ± 0.1
	Cu ₂ O-on-TiO ₂	114	14	17	1.2 ± 0.1

^{a,d} Cultured in Sabouraud CAF agar (Liofilchem, Italy) at 27°C.

^{e,g} Cultured in Nutrient agar (Liofilchem, Italy) at 27°C.

Table 1. Comparison of antimicrobial activities of Cu₂O-in-TiNT and Cu₂O-on-rutile TiO₂

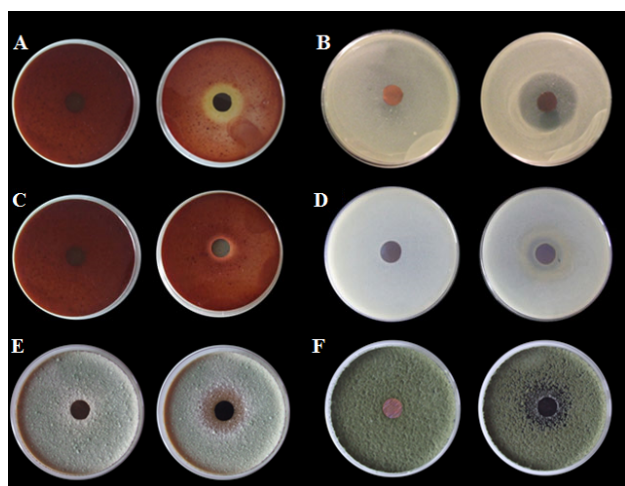


Figure 7. Zone of inhibition produced by Cu₂O-on-rutile (A, B, D) and TiO₂ Cu₂O-in-TiNT (C) specimens against the lawns of eukaryotic microorganisms: (A, C) *A. versicolor*, (B) *S. cerevisiae*, (D) *C. krusei*. In the left side - control specimen.

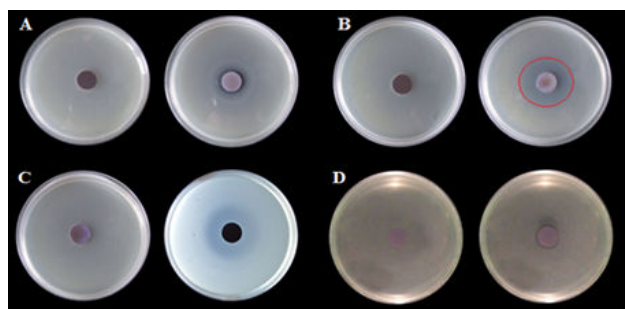


Figure 8. Zone of inhibition produced by Cu₂O-on-rutile (A, B, D) and Cu₂O-in-TiNT (C) specimens against the lawns of prokaryotic microorganisms: (A) *M. luteus*, (B, C) - *P. aeruginosa* and (D) *E. coli*. In the left side - control specimen.

The antimicrobial efficiencies of pyramidal-shaped Cu₂O species attached to various TiO₂ substrates were also assessed against typical Gram-negative (*E. coli* and *P. aeruginosa*) and Gram-positive (*M. luteus*) bacteria. Note that *P. aeruginosa* was found to be more sensitive both for Cu₂O-on-TiO₂ and Cu₂O-in-TiNT surfaces: the average inhibition zone in this bacteria lawn was 1.5 to 1.6 times wider than in *E. coli* and *M. luteus* bacteria lawns (see Table 1). We note that in contrast to Li et al.'s indication that *E. coli* is resistant to cubic and spherical Cu₂O nanocrystals [37], our Cu₂O-TiO₂ heterostructures demonstrated a strong antibacterial activity against *E. coli*. We hypothesized that differences in the antimicrobial efficacy of Cu₂O-TiO₂ heterostructures and Cu₂O nanoparticles could be explained by synergetic behaviour of p-n heterojunction between Cu₂O and TiO₂ possessing a remarkable visible light photoresponse creating OH[•] and H₂O₂ oxidative species [15] in the aqueous bacteria lawns. On the other hand, as reported by Ren et al. [23], Cu₂O octahedral single crystals bounded by {111} facets, as in our case, exhibited higher activity in killing *E. coli* than cubic ones. We also note that a similar result has been obtained under visible light illumination for *E. coli* inactivation by Cu₂O loaded on TiNT film *via* direct deposition from alkaline CuSO₄ and lactic acid solution [15].

3.3 Stability tests

To examine deterioration in photosensitivity of Cu₂O pyramidal-shaped crystals deposited from the slightly acidic Cu(II) acetate solution on the thermally oxidized Ti substrate, the stability tests were performed in a 0.5 mol L⁻¹ Na₂SO₄ solution at -0.35 V (*vs.* Ag/AgCl, sat.) and 100 W tungsten lamp illumination for up to 50 h. In these experi-

ments the tungsten lamp was placed in front of a quartz glass window of an electrochemical cell at a 12 cm distance from the socket of the lamp to the specimen. Figure 9 shows the variations in the open circuit potential of the Cu₂O-on-TiO₂ specimen after light switching before and after the stability test which lasted for 50 h. As can be seen, the Cu₂O-coated-TiO₂ specimen remained quite photosensitive to bright light even after prolonged 50 h usage. It is noteworthy that the contamination of copper ions was not detected in the tested solution even after 50 h. These results imply the prospective application of the Cu₂O-on-TiO₂ antimicrobial coatings in food and healthcare industries.

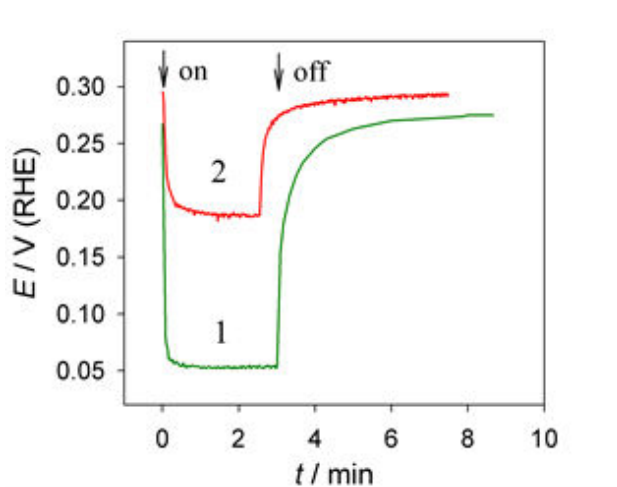


Figure 9. Variation in the open circuit potential for as formed (1) and deteriorate Cu₂O-on-TiO₂ heterostructure (2) in 0.5 mol L⁻¹ Na₂SO₄ solution after switching of light. The stability test was performed in the same solution at -0.35 V (vs Ag/AgCl, sat) under 100 W tungsten lamp illumination for 50 h.

4. Conclusions

Pyramidal-shaped pure Cu₂O crystallites were successfully deposited both in/on the TiO₂ nanotube film and onto the thermally oxidized Ti substrate by using the alternating current deposition approach from the slightly acidic copper acetate solution. Both anodized and thermally oxidized Ti surfaces after covering with pyramidal-shaped Cu₂O crystallites possess strong antimicrobial properties against the tested fungi (*A. versicolor*, *C. parapsilosis*, *C. krusei* and *S. cerevisiae*), Gram-negative (*E. coli* and *P. aeruginosa*) and Gram-positive (*M. luteus*) bacteria. In all cases, the Cu₂O-on-rutile TiO₂ surface demonstrated higher antimicrobial efficiency which could be linked with 2-3 times larger amounts of attached Cu₂O species. The antimicrobial effect of the Cu₂O species tethered to the TiO₂ surface was linked with the semiconducting properties of cuprous oxide capable of absorbing visible light and through synergetic coupling with TiO₂ produced oxidative species of OH[•] and H₂O₂ destroying the walls of microorganism cells. The Cu₂O-coated-TiO₂ specimen remained quite photosensitive to bright light even after prolonged 50 h exploitation.

5. Acknowledgements

We would like to thank Dr. V. Pakštas for XRD and Dr. Habil. G. Niaura for Raman spectra collection and comments.

6. References

- [1] Mor G K, Grimes C A (2009) TiO₂ nanotube arrays-Synthesis, Properties and Applications. Springer, New York.
- [2] Keller V, Keller N, Ledoux MJ, Lett MC (2005) Biological agent inactivation in a flowing air stream by photocatalysis. Chem. Commun. 23: 2918-2920.
- [3] Hashimoto K, Irie H, Fujishima A (2005) TiO₂ photocatalysis: a historical overview and future prospects. Jpn. J. Appl. Phys. 44: 8269-8285.
- [4] Matsunaga T, Tomoda R, Nakajima T, Wake H (1985) Photoelectrochemical sterilization of microbial-cells by semiconductor powders. FEMS Microbiol Lett. 29: 211-214.
- [5] Li G Y, Liu X L, Zhang H M, An T C, Zhang S Q, Carroll A R, Zhao H J (2011) In situ photoelectrocatalytic generation of bactericide for instant inactivation and rapid decomposition of Gram-negative bacteria. J. Catal. 277: 88-94.
- [6] Gholami M R, Elahifard M R, Rahimnejad S, Haghighi S (2007) Apatite-coated Ag/AgBr/TiO₂ visible-light photocatalyst for destruction of bacteria. J. Am. Chem. Soc. 129: 9552-9553.
- [7] Pulgarin C, Rengifo-Herrera J A, Kiwi J N (2009) S-co-doped and N-doped Degussa P-25 powders with visible light response prepared by mechanical mixing of thiourea and urea. Reactivity towards *E. coli* inactivation and phenol oxidation. J. Photoch. Photobio. 205: 109-115.
- [8] Wu P G, Xie R C, Imlay K, Shang J K (2010) Visible-light-induced bactericidal activity of titania dioxide codoped with nitrogen and silver. Environ. Sci. Technol. 44: 6992-6997.
- [9] Wu T S, Wang K X, Li G D, Sun S Y, Sun J, Chen J S (2010) Montmorillonite-supported Ag/TiO₂ nanoparticles: an efficient visible-light bacteria photodegradation material. ACS Appl. Mater. Inter. 2: 544-550.
- [10] Pang H, Gao, Lu Q (2009) Morphology effect on antibacterial activity of cuprous oxide. Chem. Commun. 1076-1078
- [11] Akhavan O, Azimirad R, Safa S, Larijani M M (2010) Visible light photo-induced antibacterial activity of CNT-doped TiO₂ thin films with various CNT contents. J. Mater. Chem. 20: 7386-7392.
- [12] Mai L X, Wang D W, Zhang S, Xie Y J, Huang C M, Zhang Z G (2010) Synthesis and bactericidal ability of Ag/TiO₂ composite films deposited on titanium plate. Appl. Surf. Sci. 257: 974-978.

- [13] Kang Q, Lu Q Z, Liu S H, Wen L X, Luo S L, Cai Q Y (2010) A ternary hybrid CdS/Pt-TiO₂ nanotube structure for photoelectrocatalytic bactericidal effects on *Escherichia coli*. *Biomaterials* 31: 3317-3326.
- [14] Hayden S C, Allam N K, El-Sayed M A (2010) TiO₂ nanotube/CdS hybrid electrodes: extraordinary enhancement in the inactivation of *Escherichia coli*. *J. Am. Chem. Soc.* 132: 14406-14408.
- [15] Hou Y, Li X Y, Zhao Q D, Quan X, Chen G H (2009) Fabrication of Cu₂O/TiO₂ nanotube heterojunction arrays and investigation of its photoelectrochemical behavior. *Appl. Phys. Lett.* 95: 093108-093111.
- [16] Zhang S, Liu C, Liu X, Zhang H, Liu P, Zhang S, Peng F, Zhao H (2012) Nanocrystal Cu₂O-loaded TiO₂ nanotube arrays films as high-performance visible-light bactericidal photocatalyst. *App. Microbiol. Biotechnol.* 96: 1201-1207.
- [17] Li H G, Dimitrevich N M, Chen L, Rajh T, Gray K A (2008) Role of surface/interfacial Cu²⁺ sites in the photocatalytic activity of coupled CuO TiO₂ nanocomposites. *J. Phys. Chem. C.* 112: 19040-19044.
- [18] Mills A, Hunte S Le (1997) An overview of semiconductor photocatalysis. *J. Photochem. Photobiol. A: Chemistry* 108: 1-35.
- [19] Garuthara R, Siripala W (2006) Photoluminescence characterization of polycrystalline n-type Cu₂O films. *J. Luminesc.* 121: 173-178.
- [20] Yang Q, Yan P X, Chang J B, Feng J J, Yue G H (2007) Growth of bicrystal CuO microsheets from aqueous solution. *Phys. Lett. A* 361: 493-496.
- [21] Zhao W Y, Fu W Y, Yang H B, Tian C J, Li M H, Li Y X, Zhang L N, Sui Y M, Zhou X M, Chen H, Zou G T (2011) Electrodeposition of Cu₂O films and their photoelectrochemical properties. *Crys. Eng. Comm.* 13: 2871-2877.
- [22] Huh A J, Kwon Y J (2011) "Nanoantibiotics": a new paradigm for treating infectious diseases using nanomaterials in the antibiotics resistant era. *J. Contr. Release* 156: 128-145.
- [23] Ren J, Wang W, Sun S, Zhang L, Wang L, Chang J (2011) Crystallography Facet-Dependent Antibacterial Activity: The Case of Cu₂O. *Ind. Eng. Chem. Res.* 50: 10366-10369.
- [24] Gerischer J H (1977) On the stability of semiconductor electrodes against photodecomposition. *J. Electroanal. Chem.* 82: 133-143.
- [25] Takeuchi M, Weichman F L, Morosawa K, Kowakami M, Nagasaka N (1988) Photoelectrochemical behavior of Cu₂O single crystals in liquid electrolytes. *Appl. Surf. Sci.* 33-34: 972-979.
- [26] De Jongh P E, Vanmaekelbergh D, Kelly J J (1999) Cu₂O: Electrodeposition and characterization. *Chem. Mater.* 11: 3512-3517.
- [27] Engel C J, Polson T A, Spado J R, Bell J M, Fillanger A (2008) Photoelectrochemistry of Porous p-Cu₂O Films. *J. Electrochem. Soc.* 155: F37-F42.
- [28] Sowers K L, Fillanger A (2009) Crystal face dependence of p-Cu₂O stability as photocathode. *J. Electrochem. Soc.* 156: F80-F85.
- [29] Jagminas A (2002) Influence of magnesium and aluminium ions on the copper a.c. deposition into aluminium anodic oxide film nanotubes. *J. Appl. Electrochem.* 32(11): 1201-1209.
- [30] Jagminas A, Kovger J, Rēza A, Niaura G, et. al. (2014) Decoration of the TiO₂ nanotube arrays with copper suboxide by AC treatment, *Electrochim. Acta* 125: 516-523.
- [31] Mikami M, Nakamura S (2002) Dynamics and dielectric properties of TiO₂ anatase: A first-principles study. *Phys. Rev. B* 66: 155213.
- [32] Ohsaka T, Izumi F, Fujiki Y (1978) Raman spectrum of anatase, TiO₂. *J. Raman Spectr.* 7: 321-325.
- [33] Yu P Y, Shen Y R (1975) Resonance Raman studies in Cu₂O. I. The phonon-assisted 1s yellow excitonic absorption edge. *Phys. Rev. B* 12: 1377-1380. *Soc.* 127: 10982-10990.
- [34] Yu P Y, Shen Y R (1975) Resonance Raman studies in Cu₂O. I. The phonon-assisted 1s yellow excitonic absorption edge. *Phys. Rev. B* 12: 1377-1381.
- [35] Carabatos C, Prevot B (1971) Rigid ion model lattice dynamics of cuprite (Cu₂O). *Phys. Status Solidi B* 44: 701-705.
- [36] Strehblow H H, Maurice V, Marcus P (2001) Initial and lateral stages of anodic oxide formation on Cu, chemical aspects, structure and electronic properties. *Electrochim. Acta* 46: 3755-3766.
- [37] Li B, Li Y, Zhao Y, Sun L (2013) Shape-controlled synthesis of Cu₂O nano/microcrystals and their antibacterial activity. *J. Phy. Chem. Solids* 74:1842-1847.